



Merging of high speed argon plasma jets

A. Case, S. Messer, S. Brockington, L. Wu, F. D. Witherspoon et al.

Citation: [Phys. Plasmas](#) **20**, 012704 (2013); doi: 10.1063/1.4775778

View online: <http://dx.doi.org/10.1063/1.4775778>

View Table of Contents: <http://pop.aip.org/resource/1/PHPAEN/v20/i1>

Published by the [American Institute of Physics](#).

Related Articles

Experimental characterization of railgun-driven supersonic plasma jets motivated by high energy density physics applications

[Phys. Plasmas](#) **19**, 123514 (2012)

Analysis of cathode geometry to minimize cathode erosion in direct current microplasma jet

[J. Appl. Phys.](#) **112**, 123302 (2012)

Practical considerations in realizing a magnetic centrifugal mass filter

[Phys. Plasmas](#) **19**, 122503 (2012)

Study of fast electron jet produced from interaction of intense laser beam with solid target at oblique incidence

[Phys. Plasmas](#) **19**, 113118 (2012)

Simulations of the linear plasma synthetic jet actuator utilizing a modified Suzen-Huang model

[Phys. Fluids](#) **24**, 113602 (2012)

Additional information on Phys. Plasmas

Journal Homepage: <http://pop.aip.org/>

Journal Information: http://pop.aip.org/about/about_the_journal

Top downloads: http://pop.aip.org/features/most_downloaded

Information for Authors: <http://pop.aip.org/authors>

ADVERTISEMENT

The advertisement banner features the 'AIP Advances' logo in green and blue, with a series of orange circles of varying sizes arranged in an arc above the text. The background is a green and white abstract pattern of flowing lines. Below the logo, the text 'Special Topic Section: PHYSICS OF CANCER' is displayed in white on a dark green background. At the bottom, the text 'Why cancer? Why physics?' is written in yellow, and a blue button with the text 'View Articles Now' is positioned on the right.

AIP Advances

Special Topic Section:
PHYSICS OF CANCER

Why cancer? Why physics? [View Articles Now](#)

Merging of high speed argon plasma jets

A. Case,¹ S. Messer,¹ S. Brockington,¹ L. Wu,¹ F. D. Witherspoon,¹ and R. Elton²

¹HyperV Technologies Corp., Chantilly, Virginia 22180, USA

²University of Maryland, College Park, Maryland 20742, USA

(Received 26 October 2012; accepted 28 December 2012; published online 15 January 2013)

Formation of an imploding plasma liner for the plasma liner experiment (PLX) requires individual plasma jets to merge into a quasi-spherical shell of plasma converging on the origin. Understanding dynamics of the merging process requires knowledge of the plasma phenomena involved. We present results from the study of the merging of three plasma jets in three dimensional geometry. The experiments were performed using HyperV Technologies Corp. 1 cm Minirailguns with a preionized argon plasma armature. The vacuum chamber partially reproduces the port geometry of the PLX chamber. Diagnostics include fast imaging, spectroscopy, interferometry, fast pressure probes, B-dot probes, and high speed spatially resolved photodiodes, permitting measurements of plasma density, temperature, velocity, stagnation pressure, magnetic field, and density gradients. These experimental results are compared with simulation results from the LSP 3D hybrid PIC code. © 2013 American Institute of Physics. [<http://dx.doi.org/10.1063/1.4775778>]

I. INTRODUCTION

The merging of high speed plasma jets is of interest both for fundamental physics studies such as laboratory models of astrophysical jets and for better understanding of the dynamics of plasma liners as compression drivers for magneto-inertial fusion.^{1–6} HyperV Technologies is developing devices capable of generating supersonic plasma jets, both advanced coaxial accelerators⁷ and Minirailguns⁸ capable of accelerating large plasma masses to velocities of tens of kilometers per second. The devices used in this series of experiments are 1 cm bore Minirailguns operating at reduced capacity compared to what can be achieved. This was done in order to guarantee large numbers of shots without significant stress on system components.

II. EXPERIMENTAL ARRANGEMENT

The experimental arrangement is shown in Figure 1. The port geometry of the end flanges of the vacuum chamber replicates the port geometry of a portion of the spherical plasma liner experiment (PLX) vacuum chamber.⁵ Three Minirailguns are placed at the corners of an equilateral triangle, aimed at the center of the chamber. The angle between any pair of guns is 37.9°. The Minirailguns were aligned using a small laser held in a fixture which fit tightly in the nozzle of the gun. A target was placed at the intended convergence point and the laser was aimed at it. The guns were aligned so that the laser spot lay within a 1 cm diameter spot on the center of the vacuum chamber.

The Minirailguns are variants of those described in Ref. 8, with a 1 cm square bore instead of 2.54 cm. The operating regime chosen was well below the maximum performance of the guns in order to ease stresses on the guns, switches, and capacitor banks. The Minirailgun consists of three subsystems: a fast gas valve, a preionizer, and a pair of tungsten alloy rails with boron nitride insulators holding them at 1 cm separation. An arc is drawn between the rails to drive a plasma armature down the length of the gun and into the

nozzle. The gas valves are a custom design which permits large masses ($\gg 10$ mg) of gas to be dispensed in a short time (≈ 400 μ s). All three gas valves are driven in parallel by a single 84 μ F capacitor bank operating at 8.5 kV and driving a current of 8 kA per valve. A ballast resistance of 0.6 Ω damped the current so as to avoid multiple openings of the valve. The preionizers were driven in parallel by a 1.2 μ F bank charged to 30 kV, with 2.2 Ω ballast resistance per preionizer. The Minirailguns were each driven by a 51 μ F capacitor bank switched by a low inductance custom switch consisting of seven pairs of electrode knobs in a linear array. Each pair of electrodes was triggered independently by a separate trigger pin. The pins were switched using a trigger fanout that triggered all pins on all switches simultaneously using a Titan 40264 spark gap switch. The rail PFNs were charged to 22 kV and typically drove a peak current of 180 kA.

A pair of fiber coupled photodiodes is used to measure initial plasma velocity by focusing collimating optics on the nozzle of one of the guns. An interferometer chord passes transversely through the chamber on center. Two spectrometer

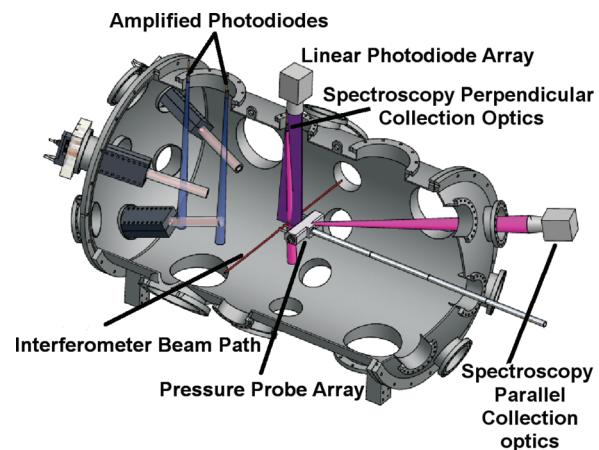


FIG. 1. Layout of the Minirailguns and diagnostics on the vacuum chamber.

chords view the center of the chamber, one at a right angle to the axis, and one at 22° off-axis, looking towards the guns. In addition, there is a 12 channel fast photodiode array viewing the merge region at the center of the chamber. This array consists of a line of fibers at the focal plane of a SLR camera, coupled to fast detection electronics in the screened control room.

In order to characterize individual gun performance, the pulse forming networks of two guns were disconnected and the remaining single gun fired while being monitored by the diagnostics. The main parameter of interest was the arrival time of the plasmoid at the center of the tank. This varied by about $1 \mu\text{s}$ per gun, compared to a total plasmoid transit time through the merge point of approximately $15 \mu\text{s}$ as measured by interferometry. In addition, interferometry showed close resemblance between the traces of all three individual Minirailguns.

The final set of parameters chosen for the merging experiments provided a plasmoid velocity of $22 \pm 2 \text{ km/s}$ as shown by spectroscopy (Figure 2) and fast photodiode measurements, and a plasmoid mass of $\sim 0.5 \text{ mg}$. The jet temperature estimated from ionization balance⁹ is approximately 1.5 eV , and the electron density is 10^{15} cm^{-3} . Because the guns were operated in off-nominal conditions, there was a small fast “prepulse” leading the main plasmoid. This does not affect the results as it has passed by the time the main plasmoid arrives at the point of convergence. The initial tests used the array of five pressure probes at three positions, at the chamber center and 12.5 cm in front of and behind center. The coordinates used are positive in the direction of plasmoid propagation. Three shots were taken at each of these positions. The probe array was then moved back, well away from the center, in order to avoid interference with interferometer and spectroscopic measurements. Finally, the probe was removed altogether and its feedthrough flange replaced with a window for axial fast imaging of the merge process.

III. RESULTS

A series of axial images of the merging process is shown in Figure 3. The bright inverted “Y” structure may be due to shocks (discussed further in Sec. IV) at the location where

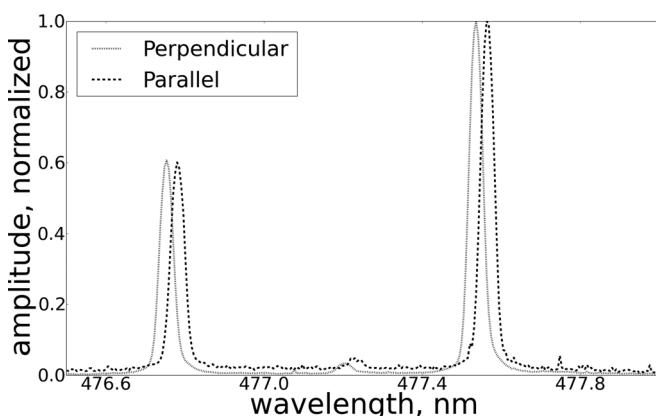


FIG. 2. Spectra taken parallel and perpendicular to the merge axis. The blue shift of the parallel spectrum corresponds to a velocity of 22 km/s . Line widths are within the experimental uncertainty of the instrumental line width, indicating temperatures below 1.5 eV .

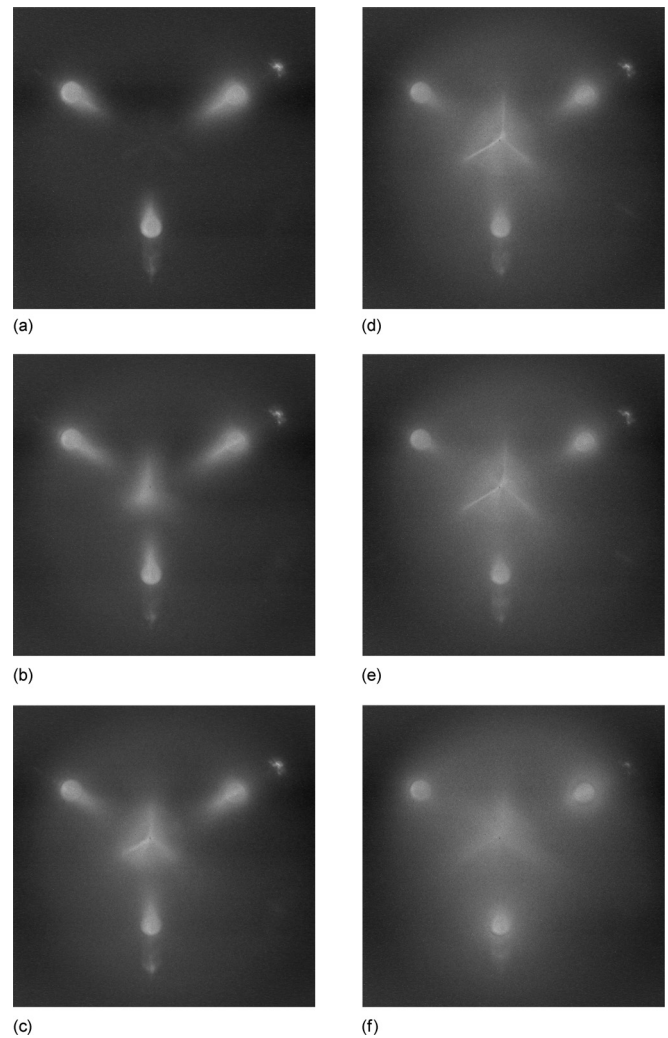


FIG. 3. Axial images of the merging process. In images (c), (d), and (e), the circular feature behind the inverted “Y” structure is caused by reflections off the center flange on the vacuum chamber. This leads to the structure appearing slightly fuzzier than it actually is. Using the nozzle exit for scale, the width of the arms of the structure is on the order of 5 mm . Exposure time is 5 ns .

the jets meet. With a convergence angle of 37.9° , the jets meet with a relative velocity perpendicular to the direction of propagation of 13.5 km/s . This corresponds to a Mach number of 5.5 in the plasma frame, which is in addition to the free expansion velocity perpendicular to the jet of $2c_s/(\gamma - 1)$. The nozzle diameter (35 mm) provides a length scale reference indicating that the thickness of the bright structures is on the order of 5 mm .

The interferometer trace for both a single jet and the merged jets is shown in Figure 4. Note that the single jet trace is magnified by a factor of ten for better visibility. It is evident from the large difference in line integrated density that the merged jets form a high plasma density region at the point of convergence. The negative swings on the interferometer trace are due to the presence of neutrals and ions. There is a detailed analysis of this effect in Ref. 10. The data in the figure are plotted in terms of line integrated density, but the single jet case is almost certain to be partially ionized. Neutrals cause a phase shift in the opposite direction from the electrons, reducing the measured density and even causing it to swing

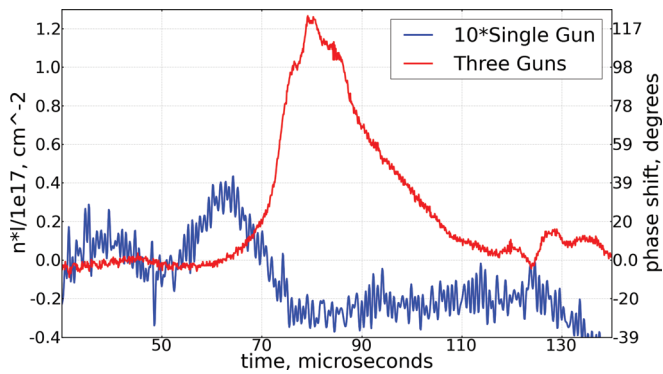


FIG. 4. Merged plasma line integrated density is far higher than single jet line integrated density, indicating compression of plasma into a compact structure at the point of convergence. Negative swings are due to neutral argon and ions. The very large electron density in the three gun case is in part due to the formation of argon III as is seen in simulations as well as to collisional ionization of neutrals as seen in the unmerged jet case.

negative as seen in the single gun case in Figure 4. Therefore, the single gun trace in its positive swing must be considered a lower bound on electron density, and in the negative portion to be dominated by neutrals. According to Ref. 10, the zero crossing of the interferometer signal occurs at an ionization fraction of approximately 0.07. To disambiguate the signal into a neutral contribution and an electron contribution would require a two color interferometer.

In order to produce the large density peak seen in the three gun case, we must assume that there is ionization of the neutrals seen in the single gun case. The center of mass merge velocity in excess of 13 km/s is sufficient to ionize argon through collisions. For this reason, we expect the peak in the three jet case to be almost fully ionized. Another factor contributing to the later peak in the three gun case is the flow of plasma into the merge region that would in the single gun case have passed on the “inside” (gun side) of the merge point. This plasma is deflected by impact with the other jets and flows into the center via a longer path than the plasma travelling directly from the nozzle. The high line integrated density in the three gun case is most likely due to the formation of a compact high density structure at the point of convergence. Imaging suggests that the width of this structure is approximately 1 cm. This implies a density of $\sim 1.2 \times 10^{17} \text{ cm}^{-3}$ in this region.

Figure 5 shows the peak pressures measured at three locations using the five fast pressure probe array. Only the center probe measured any appreciable signal though there were small signals sometimes seen on one of the off-center probes. The relatively large signal seen on the far side of the merge point is due to the impact of a collimated jet of plasma that emerges from the merge region after the jets pass through. This jet is clearly seen in images taken off the chamber axis through one of the off-axis end cap ports. Figure 6 shows such an image, taken through a port looking 22° off the chamber axis.

IV. DISCUSSION

All diagnostics indicate the formation of a compact high pressure region at the point of convergence of the three jets.

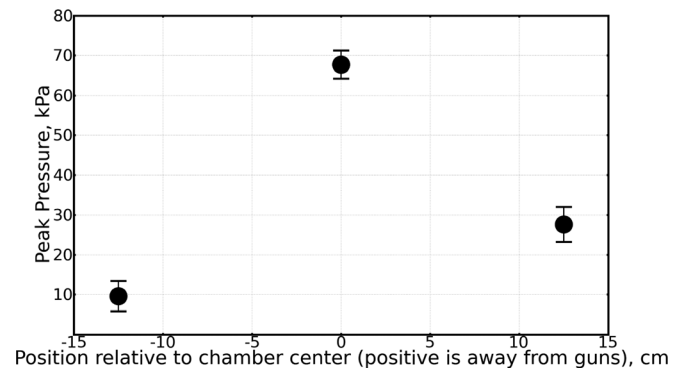


FIG. 5. Peak pressures measured at three locations, with approximate uncertainties.

As expected, there is a significant pressure spike at the point of convergence of the jets. The formation of a well collimated jet emerging from the convergence point suggests that the plasma is fairly cold even at convergence. This is consistent with the spectroscopic results and suggests that the formation of a cold, dense plasma liner for MTF applications is possible using the Minirailgun plasma accelerators.

The supersonic convergence of the jets suggests that there may be a shock at the point of intersection (the arms of the Y-shaped structure seen in Figure 3). The existing set of measurements do not provide sufficient data to test this hypothesis. Further research is ongoing as of this writing.¹¹

Simulation¹² using the LSP 3D hybrid PIC code shows the presence of narrow high density structures along the line of contact between the plasmoids as shown in Figure 7. These structures have an elevated temperature (2 eV vs 1 eV in the main plasmoid), though it must be emphasized that the simulation is of the higher performance railgun plasmoids of PLX as opposed to the lower density and lower velocity plasmoids produced by the de-rated railguns used in the present experiment. The highest temperatures measured in the current experiment are below 1.5 eV, a difference most likely due to the lower convergence velocity in this case, the PLX guns having 2.5 times the velocity. The width of the contact line structures is just under 1 cm, consistent with that seen in the images. For comparison, the ion-electron and ion-ion

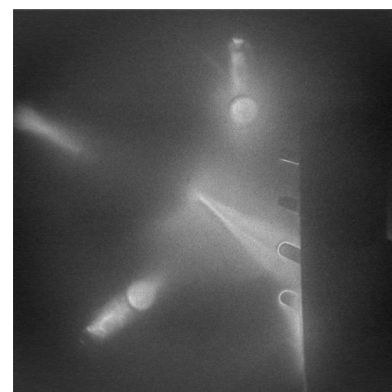


FIG. 6. Imaging off axis late in time (after peak density at merge point) shows formation of a collimated jet. The pressure probe array is seen on the right side of the image. The image is taken through the same port as the spectroscopy parallel collection optics in Fig. 1.

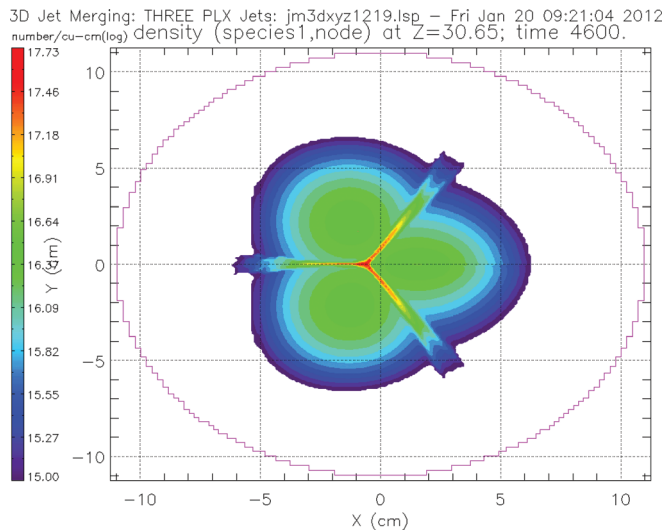


FIG. 7. A slice through a LSP simulation of three jets merging, in the plane perpendicular to the average direction of propagation of the three jets.

collision lengths are 1.5 and 0.8 cm, respectively, and the electron-ion collision length is 0.005 cm.

V. CONCLUSIONS

We have merged three plasma jets in a configuration related to that of the PLX experiment, in a parameter range lower than the PLX jets but still relevant to that experiment. We find that a compact (~ 1 cm transverse scale length), high density ($\sim 1.2 \times 10^{17}$ cm $^{-3}$), high pressure (~ 70 kPa), low temperature (~ 1.5 eV) region is formed at the point of convergence of the jets. The collision of the jets appears to result in ionization of the neutrals carried along with the plasma jet. In addition, a well collimated secondary jet emerges from the point of convergence. The line of contact between adjacent jets forms a structure which may be a shock, though further research is required to confirm this.

ACKNOWLEDGMENTS

The authors wish to acknowledge valuable discussions with Scott Hsu and Elizabeth Merritt.

Research supported by the DOE Office of Fusion Energy Science under Grant No. DE-FG02-05ER54810 and SBIR Grant No. DE-FG02-08ER85114.

Work supported by the United States Department of Energy Office of Fusion Energy Sciences.

- ¹Y. C. F. Thio, C. E. Knapp, R. C. Kirkpatrick, R. E. Siemon, and P. Turchi, "A physics exploratory experiment on plasma liner formation," *J. Fusion Energy* **20**, 1 (2001).
- ²Y. C. F. Thio, E. Panarella, R. C. Kirkpatrick, C. E. Knapp, and F. Wysocki, "Magnetized target fusion in spheroidal geometry with standoff drivers," in *Proceedings of the 2nd Symposium on Current Trends in International Fusion Research*, edited by E. Panarella (NRC of Canada Research, Ottawa, 1999), pp. 113–134.
- ³J. Loverich and A. Hakim "Two-dimensional modeling of ideal merging plasma jets," *J. Fusion Energy* **29**, 532–539 (2010).
- ⁴S. A. Galkin, I. N. Bogatu, and J. S. Kim, "High density high velocity plasma jet interaction," in *Proceedings of the 16th IEEE International Pulsed Power Conference* (2007), pp. 947–950.
- ⁵S. C. Hsu, T. J. Awe, S. Brockington, A. Case, J. T. Cassibry, G. Kagan, S. J. Messer, M. Stanic, X. Tang, D. R. Welch, and F. D. Witherspoon, "Spherically imploding plasma liners as a standoff driver for magneto-inertial fusion," *IEEE Trans. Plasma Sci.* **40**(5), 1287 (2012).
- ⁶J. H. Degnan, W. L. Baker, M. Cowan, Jr, J. D. Graham, J. L. Holmes, E. A. Lopez, D. W. Price, D. Ralph, and N. F. Roderick, "Operation of a cylindrical array of plasma guns," *Fusion Technol.* **35**, 354–360 (1999).
- ⁷F. D. Witherspoon *et al.*, "A contoured gap coaxial plasma gun with injected armature," *Rev. Sci. Instrum.* **80**, 083506 (2009).
- ⁸F. D. Witherspoon, R. Bomgardner, S. Brockington, A. Case, S. Messer, D. Van Doren, L. Wu, and R. Elton, "Minirailgun plasma jet accelerators for HEDLP and fusion applications," *Rev. Sci. Instrum.* (submitted).
- ⁹H.-K. Chung, M. H. Chen, W. L. Morgan, Y. Ralchenko, and R. W. Lee, *High Energy Density Phys.* **1**, 3–12 (2005).
- ¹⁰E. C. Merritt, A. G. Lynn, M. A. Gilmore, C. Thoma, J. Loverich, and S. Hsu, "Multi-chord fiber-coupled interferometry of supersonic plasma jets and comparisons with synthetic data," *Rev. Sci. Instrum.* **83**, 10D523 (2012).
- ¹¹S. Messer, A. Case, L. Wu, S. Brockington, and F. D. Witherspoon, "Nonlinear compressions in merging plasma jets" (unpublished).
- ¹²L. Wu, M. Phillips, and F. D. Witherspoon, "Numerical simulation of merging plasma jets using high-Z gases," *IEEE Trans. Plasma Sci.* (submitted).